Pressure-Induced Phase Transition in Hydrogen-Bonded Supramolecular Structure: Guanidinium Nitrate

Run Wang,[†] Shourui Li,[†] Kai Wang,[†] Defang Duan,[†] Lingyun Tang,[‡] Tian Cui,[†] Bingbing Liu,[†] Qiliang Cui,[†] Jing Liu,[‡] Bo Zou,*[,†] and Guangtian Zou[†]

State Key Laboratory of Superhard Materials, Jilin University, Changchun 130012, P. R. China, and Beijing Synchrotron Radiation Laboratory, Institute of High Energy Physics, Chinese Academy of Sciences, Beijing 100039, P. R. China

Received: September 08, 2009; Revised Manuscript Received: April 22, 2010

In situ Raman scattering and synchrotron X-ray diffraction have been used to investigate the effects of high pressure on the structural stability of guanidinium nitrate ($C(NH_2)_3^+ \cdot NO_3^-$, GN), a representative two-dimensional supramolecular architecture of hydrogen-bonded rosette network. This study has confirmed a structural phase transition observed by Raman scattering and X-ray diffraction at ~1 GPa and identified it as a space group change from $C2$ to $P2_1$. The high-pressure phase remained stable up to 22 GPa. We discussed the pressure-induced changes in N−H stretching vibration in Raman spectra and proposed that this phase transition is due to the rearrangements of the hydrogen-bonding networks.

Introduction

Supramolecular chemistry has provided a wide canvas for a variety of studies of molecular materials in the solid state.[1−3] Supramolecular interactions, which include hydrogen bonding, play a vital role in the design of supramolecular architectures.[4] The contribution of hydrogen bonds to the area of supramolecular chemistry is definitely outstanding owing to the reversibility, specificity, directionality, and better tuning of stabilization.[5−8] The hydrogen-bonding interactions between the individual building blocks and the resulting lattice architecture substantially determine the properties of supramolecules. Moreover, hydrogen bonds which define the aggregation state can be easily altered by compression as the Coulombic interaction between the protons and acceptor atoms is relatively weak compared to covalent bonds.[9−11] This means that pressure has the ability to control the strength of hydrogen-bonding interaction. Thus, the study of hydrogen bonds under high pressure can give valuable information to probe the stability of the supramolecular system.

Pressure is suitable for altering hydrogen bonding, as small variations in the applied forces typically results in large changes in intermolecular separations, which often trigger dramatic reorganization of crystal packing,[12,13] without encountering the major perturbations produced by changes in temperature and chemical composition.[14] In order to obtain reliable structural information under high pressure, *in situ* angle dispersive X-ray diffraction (ADXD) patterns with high-intensity synchrotron radiation have been applied to high-pressure diffraction experiments with a diamond anvil cell (DAC). Raman spectroscopy could also provide a fundamental method to indentify phase transitions and analyze variations in hydrogen bonding. Recently, pressure-induced phase transitions in hydrogen-bonded proteins and amino acids have been addressed in the literature.[15,16] In our previous work on supramolecules, the cyanuric acid−melamine adduct underwent an irreversible phase transition under high pressure,[17] while in the hydrogen-bonded supramolecular adduct formed by melamine and boric acid, a reversible pressure-induced amorphization was observed.[18]

Guanidinium nitrate ($C(NH_2)_3^+ \cdot NO_3^-$, GN) is a representative supramolecular architecture of hydrogen-bonded rosette network which is built of sheets of guanidinium and nitrate ions linked by N−H···O hydrogen bonds.[19−21] According to the reports, GN crystals reveal two temperature-induced phase transition. The low-temperature phase, GN1, on heating at $T_{12} = 296$ K, undergoes a transition to phase GN2. Then a continuous phase transition happens at $T_{23} = 384$ K, with the crystals transforming to GN3 phase.[22,23] The structures of these three phases are two-dimensional hydrogen-bonded layer motifs with different space groups at ambient pressure.[21] The GN2 phase exists at ambient condition and has a monoclinic structure belonging to $C2$ space group with the unit cell parameters $a = 12.545(5)$ Å, $b = 7.303(4)$ Å, $c = 7.476(4)$ Å, and $\beta = 124.93(5)°$ at 292 K (see Figure 1). Because of its relative simple structure, GN2 can be considered as a model system for us to investigate the influence of high pressure on the hydrogen-bonded supramolecular structures. Furthermore, the structure and stability of GN2 at high pressure are determined mainly by the balance between hydrogen-bonding and electrostatics interaction.[21] Therefore, high-pressure studies on GN2 are also valuable for comprehending the relationship between long-range electrostatics forces and geometric factors.

In the present paper, we have performed *in situ* XRD as well as Raman spectroscopy measurements to detect the phase transition and the motions of molecular fragments in crystalline GN2 at high pressure. It is interesting to see which consequences the hydrogen bonds will have for the stability of the structure with respect to phase transitions. Besides, we are particularly concerned with the mechanisms of the structural phase transition and the structural information on high-pressure phase. These studies provide a better understanding of the nature of the hydrogen bonding and structural stability of the supramolecular architectures under high pressure.

* Corresponding author. E-mail: zoubo@jlu.edu.cn.
[†] Jilin University.
[‡] Chinese Academy of Sciences.

10.1021/jp908656m
Published on Web 04/30/2010

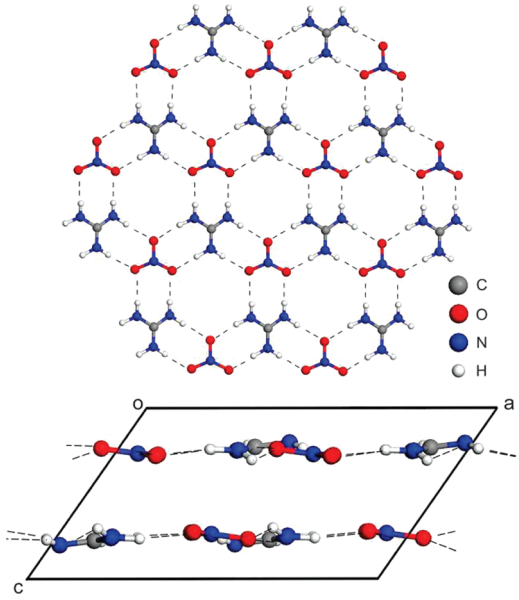

Figure 1. Top: one sheet of hydrogen-bonded rosette network in GN2; dashed lines represent interionic hydrogen bonds. Bottom: crystal structure of GN2 along crystallographic *b* axis. Color legend: carbon (gray), oxygen (red), nitrogen (blue), hydrogen (white).

Experimental Section

Guanidinium nitrate (GN) was purchased from Sigma-Aldrich Co. Powder samples used for the ambient measurements (Raman, XRD) were prepared by crushing single crystals using a mortar. Because the temperature-induced transformation from GN1 to GN2 showed a 20 K temperature hysteresis, the experimental temperature was held constant at 297 K to ensure samples in GN2 phase.[23]

GN2 along with a few grains of ruby pressure calibrant was loaded in a 150 μm diameter hole of an 80 μm thick T301 stainless steel gasket and pressurized using a Mao-Bell type DAC. In case of layer structure of GN2, which makes it a very soft material, no pressure medium was employed,[24] and the ruby lines were found to be sharp and well separated to the highest pressure of 20 GPa. Thus, we confirmed quasi-hydrostatic conditions over the whole pressure range.[25]

Raman spectra with the DAC were recorded in the backscattering geometry, using the Renishaw System (inVia Raman microscope) with a 514.5 nm argon ion laser as the excitation source, and the laser power was kept at 10 mW. Prior to each measurement, the spectrometer was calibrated using the Si line. The resolution of the system was about 1 cm^{-1}. The Raman spectra were collected in the ranges of 100−1150 and 3000−3600 cm^{-1} as a function of pressure.

Angle-dispersive X-ray diffraction measurements were carried out on 4W2 High Pressure Station of Beijing Synchrotron Radiation Facility (BSRF). Monochromatic radiation at a wavelength of 0.6199 Å was adopted for pattern collection. Portions of angle-dispersive X-ray diffraction measurements were performed at 16IDB of the HPCAT (high-pressure collaborative access team) at the Advanced Photon Source in Argonne National Laboratory. Diffraction images were recorded with a Mar345 image plate detector and were integrated and corrected for distortions using the FIT2D software.[26] The X-ray diffraction peak positions of GN2 samples were determined by fitting the pattern with a combination of Gaussian and Lorentzian functions and analyzed using the Material Studio program.

Ab initio calculations were performed with the pseudopotential plane-wave method based on density functional theory implemented in the CASTEP code. The local density approximation exchange-correlation functional was used in the calculations. Vanderbilt-type ultrasoft pseudopotentials were employed with a plane-wave cutoff energy of 300 eV.

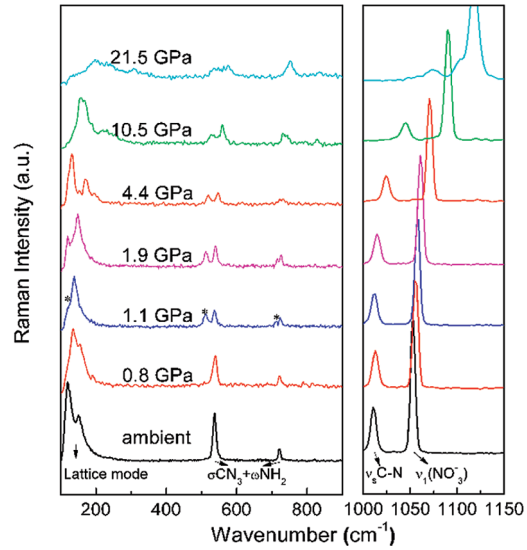

Figure 2. Selected Raman spectra of GN2 as a function of increasing pressure in the wavenumber range 100−1150 cm^{-1}. The curves in this figure are vertically displaced for the sake of clarity.

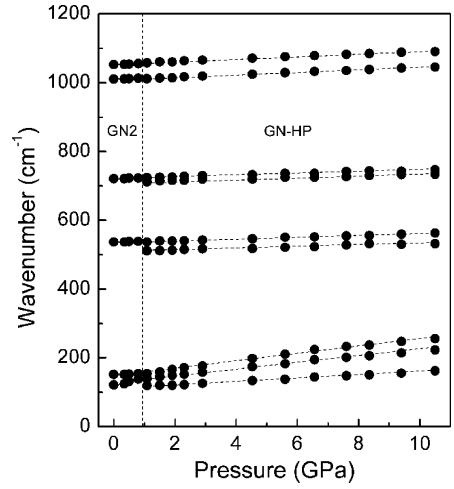

Figure 3. Pressure-induced shifts of lattice modes and internal modes in the range of 100−1200 cm^{-1}. Linear fits are shown for the frequency shifts. The vertical dashed line marks the onset of discontinuity.

Results and Discussion

Pressure-induced changes in the internal and external modes in the frequency range 100−1150 cm^{-1} under different pressures are shown in Figure 2. Band assignments for the vibrations of GN1 were based on a reported experimental and theoretical study.[27,28] The patterns of Raman spectra of GN1 and GN2 were found to be identical at ambient pressure ranging from 100 to 3600 cm^{-1}. Therefore, the band assignments for the vibrations of GN1 were feasible for GN2. The shifts of these modes as a function of observed pressure are depicted in Figure 3. We labeled the lattice modes legibly in Figure 4 to reveal the variation trends and emergence of lattice modes with increasing pressure.

As seen in Figures 2 and 3, we were able to distinguish two lattice modes below 200 cm^{-1} at ambient pressure from the low-frequency spectrum. These modes were very sensitive to subtle

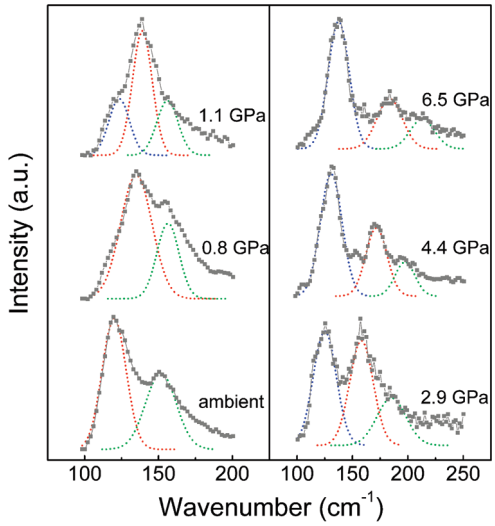

Figure 4. Decomposition of bands related to the lattice modes at different pressures.

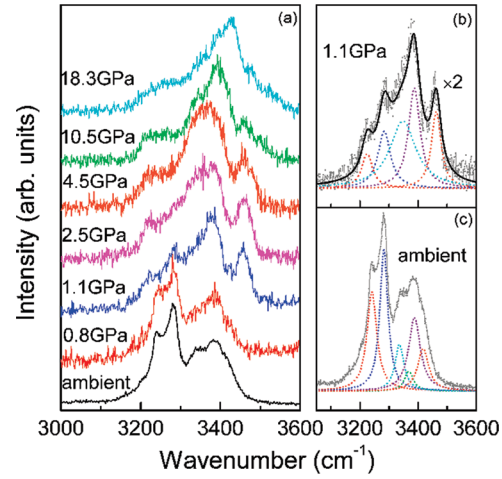

Figure 5. (a) Selected Raman spectra of GN2 as a function of increasing pressure in the N−H stretching frequency region. (b) and (c) show the decomposition of N−H stretching bands at ambient pressure and 1.09 GPa with Lorentz function, respectively.

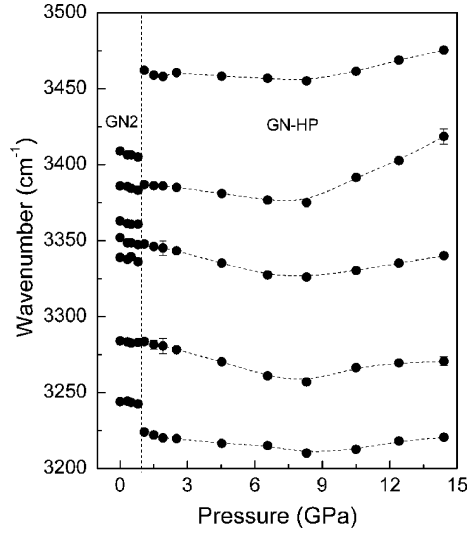

Figure 6. Pressure-induced shifts for N−H stretching modes. Error bars are given where errors are larger than the size of symbol. The vertical dashed line marks the onset of discontinuity.

changes upon application of pressure due to the weak interionic interaction.[29,30] Raman bands of lattice modes situated at 121 and 153 cm^{-1} exhibited a slight blue shift in lower-pressure range, which implied that these mode hardenings before 1.1 GPa clearly represented the enhancement of interion interactions.[31] Nevertheless, the band at 153 cm^{-1} was not as sensitive to pressure as the one at 121 cm^{-1}. This fact were deduced from the only participation of the guanidinium cation in this libration.[27]

However, considerable changes in the spectrum were observed such as the appearance of new modes and splitting of existing modes at 1.1 GPa. As seen from Figures 2 and 3, there was a lattice mode arising at 117 cm^{-1}. At the same time, the bands (540 and 724 cm^{-1} at ambient pressure) related to CN_3 deformation motion and NH_2 bending showed markedly 2-fold splitting. With further increase of pressure up to 21.5 GPa, spectrum remains essentially similar to that at 1.1 GPa. The large variations in Raman spectra demonstrated that a pressure-induced phase transition occurred at room temperature near 1 GPa. The new phase will be named the GN-HP phase. The splitting of bands (internal modes) in Raman spectra was indicative of lowering molecular and/or crystal symmetry due to the phase transition.[32] Beyond the phase transition, all of Raman bands in this internal region exhibited shifts toward to the high frequencies owing to the decrease in the bond distance and increase in the effective force constants.[33]

Figure 5 illustrates the observed Raman spectra of the NH_2 stretching vibrations at several pressures, together with the decompositions of bands corresponding to the NH_2 stretching vibrations at ambient pressure and 1.1 GPa, respectively. The pressure-induced shifts of the NH_2 stretching modes are shown in Figure 6. According to the assignment in ref 27, the bands (3409, 3386, 3363, 3352, and 3334 cm^{-1}) are assigned to asymmetric NH_2 stretching vibrations at ambient pressure, while 3284 and 3240 cm^{-1} corresponding to symmetric stretching vibrations. In contrast to the other modes, these stretching frequencies of all N−H bonds initially slightly decreased up to 1.1 GPa. The red shifts were in accordance with general rules that an increase of pressure decreases the D−H stretching frequencies of weak and moderate strength D−H···A bonds.[34−36] The N−H bond length was extended by the increasing electrostatic attraction between H···O with compression, thus reducing the frequency of N−H stretching vibration. This pressure effect could be attributed to an increase in the N−H···O hydrogen bond strength under pressure. When the pressure went beyond 1.1 GPa, from Figure 5 we could observe that NH_2 stretching modes exhibited obvious changes in intensity and position. The phase transition was also apparent owing to the emergence of these new five bands related to NH_2 stretching vibrations.

With further increase of pressure, all of NH_2 stretching modes remained undergoing a considerable red shift up to ~8 GPa, which indicated that hydrogen bonds between neighboring molecules still existed in GN-HP phase and all the N−H bonds participated in hydrogen bonds as before. At the same time, the application of pressure resulted in a continuous increase in the N−H···O hydrogen bond strength. However, at ~8 GPa these frequencies suddenly started to increase at different rates of pressure shifts (see Figure 6). During this process the relative intensity of the band at 3346 cm^{-1} was found to increase considerably with compression until ~6 GPa. When this mode started to move to a higher frequency, it was observed to be a shoulder of the most intense band adjacent to it. Concomitantly, the band at 3281 cm^{-1} moved into the lower frequency band (3225 cm^{-1}), and these two modes exhibited a blue shift together

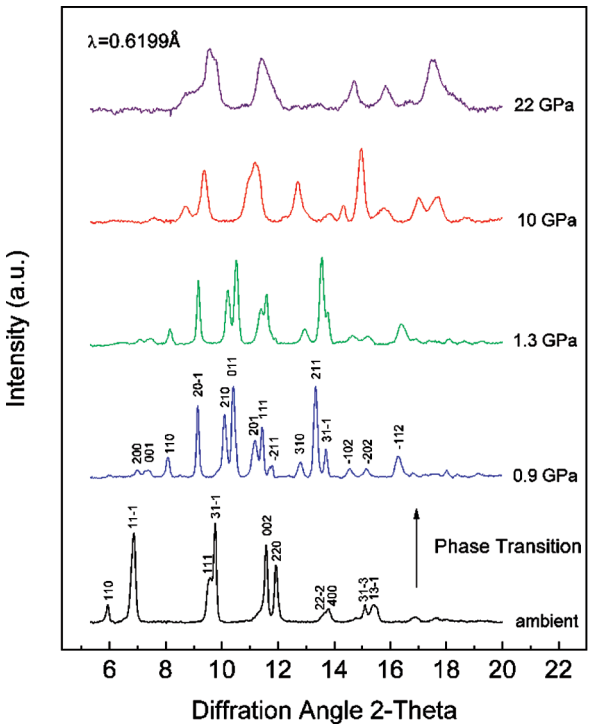

Figure 7. Representative X-ray diffraction patterns of GN2 after baseline corrections at different pressures.

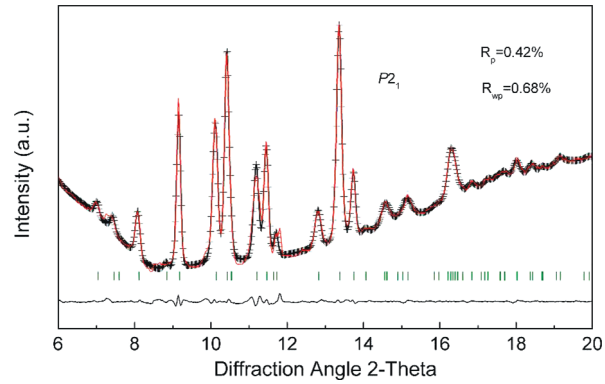

Figure 8. XRD patterns at 0.9 GPa: red line, experiment; dotted line, computer-generated diffraction pattern for the $P2_1$ structure; the lower curve is the fit residual.

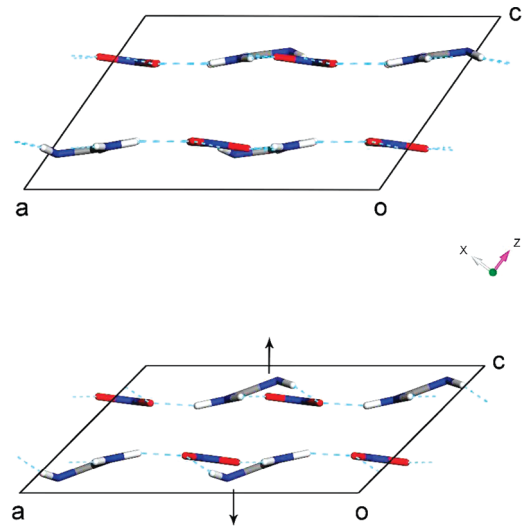

Figure 9. Crystal structures of GN2 at ambient pressure (up) and high pressure (down) along crystallographic *b* axis. The arrows indicate the displacement of guanidinium cations.

after compression to ~5 GPa. The blue shift was primarily due to the significant enhancement of hydrogen bond strength. Compounds with strong, symmetrical hydrogen bonds exhibited a different behavior, with the D−H stretching modes typically shifting to higher frequencies with increasing pressures.[37] Thus, N−H bonds participated in strong hydrogen bonds at higher pressure.

The geometry of hydrogen bond can be distorted very easily under high pressure. At sufficiently high pressure (~1 GPa), the increased energy of interionic interactions may rotate ions or molecular fragments and distorted the hydrogen-bonded networks.[38] The observed abrupt changes of the N−H stretching modes at ~1 GPa implied that there was a considerable rearrangement of hydrogen bonds. Fortunately, the hydrogen-bonded framework of GN crystal was preserved through the phase transition.

For a further understanding of the GN2 transition caused by pressure, it is necessary to obtain X-ray diffraction data. The evolution of the representative X-ray diffraction patterns to 22 GPa is shown in Figure 7. As can be seen, an abrupt change of the diffraction pattern, which is the most convincing evidence for the pressure-induced phase transition, was observed at 0.9 GPa. This change in diffraction pattern occurred in the same pressure region where the modification of N−H stretching modes and CN_3 deformation modes were observed in Raman spectrum. We believed that it was a new phase compared to the XRD patterns of the other two temperature-induced phases of GN.[21] Above 0.9 GPa, as evident from Figure 2, the diffraction peaks shifted to higher angles with uploading pressure, indicating a decrease of interplanar distance of crystal planes. With increasing pressure, the GN-HP phase remained stable up to the highest pressure (Figures S1 and S2).

All of the subsequent XRD patterns above 0.9 GPa were best described with monoclinic symmetry, and the indexed lattice parameters were $a = 10.35(5)$ Å, $b = 4.88(7)$ Å, $c = 4.88(8)$ Å, and $\beta = 101.42(6)°$, with unit cell volume $V = 242.46$ Å^3 at 0.9 GPa. The intensity refinements of the X-ray diffraction data suggested that the most likely structure of high-pressure phase was in space group $P2_1$ (see Figure 8). It is obvious that there were considerable reductions on volume of crystal cell and lattice parameters in high-pressure phase compared to GN2, which implies that the ions are more efficiently packed in high-pressure phase. In comparison with the ambient space group, the high-pressure space group $P2_1$ had lower symmetry than $C2$. The symmetry lowering of high-pressure crystal structure provided a circumstantial evidence for the splitting of Raman modes in the Raman spectra of GN-HP phase. Moreover, in contrast to the low-temperature phase GN1 which crystallizes in *Cm* space group, ions adopt different relative orientation in the GN-HP phase, which led to a more complicated crystal structure. However, most interestingly, the symmetry of GN2 crystal increased when crystal heated to T_{23}: from space group $C2$ in GN2 to $C2/m$ in the GN3 phase.

To understand what changes are happening of hydrogen-bonding networks under high pressure, we performed *ab initio* calculations with the pseudopotential plane-wave method based on density functional theory. The details of calculations are stated in the Supporting Information. The calculated results revealed that the hydrogen-bonded sheet was distorted to wave-shaped structure at higher pressure (Figures 9 and 10). It is worthy to note that guanidinium cations (marked by the shadow in Figure 10) were modulated into tilt and displacement from the average plane of sheet, while the separation between the sheets became decreased. On the basis of the calculated

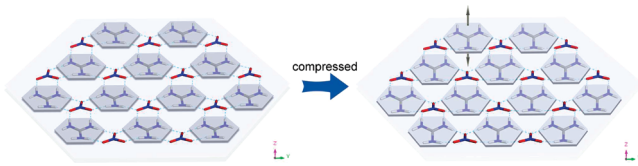

Figure 10. Changes of guanidinium cations in two-dimensional hydrogen-bonded planar sheet.

hydrogen-bonding model, we propose the following mechanism for the phase transition.

Hydrogen-bonding and electrostatic forces are the predominant interactions between guanidinium cations and nitrate anions. The pressure-induced phase transition can be understood from the layer structure of GN2 crystal and the balance between hydrogen-bonding and electrostatic forces. On the one hand, owing to the high pressure the neighboring sheets in the crystal become closer to each other inevitably, which results in an increase in electrostatic interactions between them.[23] The arrangement of the sheets is destabilized by increasing electrostatic forces between near pairs of the sheets, which must be compensated for by attracting electrostatic interactions with further layers of ions and by dispersion forces. Therefore, with increasing pressure the ions becomes gradually tilted and displaced from the average plane of sheet to reduce repulsive electrostatic interactions between near sheets.[21] On the other hand, the interionic hydrogen-bonding interactions and electrostatic forces within each layer are also strengthened with the reduction of distance between the ions in the layers under high pressure. On further compression, the balance between hydrogen-bonding interactions and electrostatic forces within sheets are disturbed due to not only the nonideal symmetric planar layers but also the competition between these two interionic interactions. At sufficiently high pressures (~1 GPa), the sheets of hydrogen-bonded ions can no longer afford the increased inter- and intralayer interionic interactions. Thus, the phase transition and rearrangement of hydrogen-bonding network occur to reduce the total energy, forcing ions to move to new equilibrium positions.

The features observed in Raman spectra under high pressure are consistent with the proposed mechanism of this phase transition, and the spectrum can also show some details of phase transition. Before phase transition the red shifts of all N−H stretching modes reveal the strengthening of hydrogen bonds within sheets. At ~1 GPa, the large changes in the N−H stretching modes suggest a substantial modification of the hydrogen-bonding networks. Furthermore, the significant splitting of CN_3 deformation vibrations exhibits the rearrangement of guanidinium cations. Because the lattice modes are affected by pressure as well, the phase transition involves structural modification of both the ions and their arrangement. However, further high-pressure neutron diffraction studies are required to provide reliable information on the hydrogen atomic positions.

Conclusion

We have performed high-pressure studies of GN2 crystal using Raman spectroscopy and synchrotron X-ray diffraction. Both Raman and X-ray diffraction data indicated the occurrence of phase transitions at ~1 GPa, and the high-pressure phase was found to be stable up to 22 GPa. The X-ray diffraction data confirmed the structure of high-pressure phase changed from $C2$ to $P2_1$ symmetry. Moreover, the behavior N−H stretching vibration in Raman spectra demonstrated the existence of hydrogen bonds in high-pressure phase. In addition, the phase transition was companied by the modification and rearrangement of the hydrogen-bonding network. These studies will be important to further develop an understanding of hydrogen bonds and stability of hydrogen-bonded supramolecular systems under high-pressure conditions.

Acknowledgment. The authors are grateful to Dr. Ho-kwang Mao and Dr. Yue Meng for help on experiments. This work is supported by NSFC (Nos. 20773043, 20673048, and 10674053), the National Basic Research Program of China (Nos. 2005CB724400 and 2007CB808000), and Project 20080108 Supported by Graduate Innovation Fund of Jilin University. This work was performed at 4W2 HP-Station, Beijing Synchrotron Radiation Facility (BSRF) which is supported by Chinese Academy of Sciences (No. KJCX2-SW-N20KJCX2-SW-N03).

Supporting Information Available: Raman spectra and X-ray diffraction patterns between 10 and 22 GPa (Figures S1 and S2) and details of *ab initio* calculations. This material is available free of charge via the Internet at http://pubs.acs.org.

References and Notes

(1) Lawrence, D. S.; Jiang, T.; Levett, M. *Chem. Rev.* **1995**, *95*, 2229.
(2) Lehn, J. M. *Science* **1985**, *227*, 849.
(3) Whitesides, G. M.; Grzybowski, B. *Science* **2002**, *295*, 2418.
(4) Ward, M. D. *Chem. Commun.* **2005**, 5838.
(5) Han, J.; Yau, C.-W.; Lam, C.-K.; Mak, T. C. W. *J. Am. Chem. Soc.* **2008**, *130*, 10315.
(6) Kohmoto, S.; Kuroda, Y.; Someya, Y.; Kishikawa, K.; Masu, H.; Yamaguchi, K.; Azumaya, I. *Cryst. Growth Des.* 2009.
(7) Prins, L. J.; Reinhoudt, D. N.; Timmerman, P. *Angew. Chem., Int. Ed.* **2001**, *40*, 2382.
(8) MacDonald, J. C.; Whitesides, G. M. *Chem. Rev.* **1994**, *94*, 2383.
(9) Boldyreva, E. *Acta Crystallogr. A* **2008**, *64*, 218.
(10) Goncharov, A. F.; Manaa, M. R.; Zaug, J. M.; Gee, R. H.; Fried, L. E.; Montgomery, W. B. *Phys. Rev. Lett.* **2005**, *94*, 065505.
(11) Lee, K. M.; Chang, H. C.; Jiang, J. C.; Chen, J. C. C.; Kao, H. E.; Lin, S. H.; Lin, I. J. B. *J. Am. Chem. Soc.* **2003**, *125*, 12358.
(12) Dreger, Z. A.; Gupta, Y. M.; Yoo, C. S.; Cynn, H. *J. Phys. Chem. B* **2005**, *109*, 22581.
(13) Park, T. R.; Dreger, Z. A.; Gupta, Y. M. *J. Phys. Chem. B* **2004**, *108*, 3174.
(14) Bridgman, P. W. *Proc. Am. Acad. Arts Sci.* **1911**, *47*, 441.
(15) Potekhin, S. A.; Senin, A. A.; Abdurakhmanov, N. N.; Tiktopulo, E. I. *Biochim. Biophys. Acta* **2009**, *1794*, 1151.
(16) Minkov, V. S.; Krylov, A. S.; Boldyreva, E. V.; Goryainov, S. V.; Bizyaev, S. N.; Vtyurin, A. N. *J. Phys. Chem. B* **2008**, *112*, 8851.
(17) Wang, K.; Duan, D. F.; Wang, R.; Liu, D.; Tang, L. Y.; Cui, T.; Liu, B. B.; Cui, Q. L.; Liu, J.; Zou, B.; Zou, G. T. *J. Phys. Chem. B* **2009**, *113*, 14719.
(18) Wang, K.; Duan, D. F.; Wang, R.; Lin, A. L.; Cui, Q. L.; Liu, B. B.; Cui, T.; Zou, B.; Zhang, X.; Hu, J. Z.; Zou, G. T.; Mao, H. K. *Langmuir* **2009**, *25*, 4787.
(19) Katrusiak, A.; Szafranski, M. *Acta Crystallogr. C* **1994**, *50*, 1161.
(20) Szafranski, M.; Katrusiak, A. *Chem. Phys. Lett.* **2004**, *391*, 267.
(21) Katrusiak, A.; Szafranski, M. *J. Mol. Struct.* **1996**, *378*, 205.
(22) Szafranski, M. *Solid State Commun.* **1992**, *84*, 1051.
(23) Szafranski, M.; Czarnecki, P.; Dollhopf, W.; Hohne, G. W. H.; Brackenhofer, G.; Nawrocik, W. *J. Phys.: Condens. Matter* **1993**, *40*, 7425.
(24) Rao, R.; Sakuntala, T.; Godwal, B. K. *Phy. Rev. B* **2002**, *65*, 054108.
(25) Rao, R.; Sakuntala, T.; Arora, A. K.; Deb, S. K. *J. Chem. Phys.* **2004**, *121*, 7320.
(26) Hammersley, A. P.; Svensson, S. O.; Hanfland, M.; Fitch, A. N.; Hausermann, D. *High Press. Res.* **1996**, *14*, 235.
(27) Szafranski, M. *Phys. Status Solidi B* **1997**, *201*, 343.
(28) Drozd, M. *Mater. Sci. Eng., B* **2007**, *136*, 20.
(29) Kavitha, G.; Narayana, C. *J. Phys. Chem. B* **2006**, *110*, 8777.
(30) Banerji, A.; Deb, S. K. *J. Phys. Chem. B* **2007**, *111*, 10915.
(31) Ciezak, J. A.; Jenkins, T. A.; Liu, Z.; Hemley, R. J. *J. Phys. Chem. A* **2007**, *111*, 59.
(32) Dreger, Z. A.; Gupta, Y. M. *J. Phys. Chem. B* **2007**, *111*, 3893.
(33) Orgzall, I.; Franco, O.; Schulz, B. *J. Phys.: Condens. Matter* **2006**, *18*, 5269.
(34) Hamann, S.; Linton, M. *Aust. J. Chem.* **1975**, *28*, 2567.
(35) Moon, S. H.; Drickamer, H. G. *J. Chem. Phys.* **1974**, *61*, 48.
(36) Reynolds, J.; Sternstein, S. S. *J. Chem. Phys.* **1964**, *41*, 47.
(37) Custelcean, R.; Dreger, Z. A. *J. Phys. Chem. B* **2003**, *107*, 9231.
(38) Boldyreva, E. V. *J. Mol. Struct.* **2004**, *700*, 151.

JP908656M